MDDC - 485
LADC - 132

UNITED STATES ATOMIC ENERGY COMMISSION

CERTAIN NEUTRON PROPERTIES OF MATERIALS

Part I

LIBRARY OF CONGRESS
SCIENCE & TECHNOLOGY PROJECT
TECHNICAL INFORMATION SECTION

DEC 7 1948

by

H. Barschall
E. Graves
J. H. Manley
V. F. Weisskopf

Los Alamos Scientific Laboratory

DISTRIBUTION STATEMENT A
Approved for public release
Distribution Unlimited

Date of Manuscript: January 15, 1944
Date Declassified: November 18, 1946

Issuance of this document does not constitute authority for declassification of classified copies of the same or similar content and title and by the same author.

Technical Information Division, Oak Ridge Operations
AEC, Oak Ridge, Tenn., 11-15-48--850-12503

Printed in U.S.A.
PRICE 15 CENTS

DTIC QUALITY INSPECTED 1

19961011 121

DISCLAIMER NOTICE

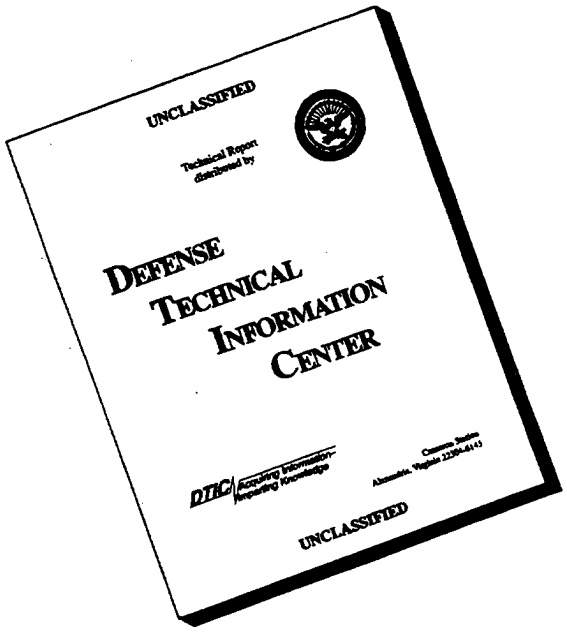

THIS DOCUMENT IS BEST QUALITY AVAILABLE. THE COPY FURNISHED TO DTIC CONTAINED A SIGNIFICANT NUMBER OF PAGES WHICH DO NOT REPRODUCE LEGIBLY.

CERTAIN NEUTRON PROPERTIES OF MATERIALS

Part I

By H. Barschall, E. Graves, J. H. Manley, and V. F. Weisskopf

ABSTRACT

Measurements are being made of the transport cross section and inelastic scattering cross section for fast neutrons of various energies in various materials. This is the first of a series of reports in which the results are to be reported and discussed. It includes measurements of back scattering and poor-geometry transmission scattering for neutrons of 1.5 and 3 Mev.

A. INTRODUCTION

The present experiments have as their purpose the measurement of the transport mean free path, i.e., the reciprocal of the transport cross section times the number of nuclei per unit volume. The transport cross section σ_t is defined by

$$\sigma_t = \int_0^{\pi} \sigma(\theta)\ (1 - \cos\theta)\ \sin\theta\ d\theta$$

where θ is the scattering angle and $\sigma(\theta)$ the total scattering cross section per unit solid angle, i.e., the sum of the cross sections for elastic and inelastic scattering.

The energy loss in inelastic scattering of the neutrons is investigated by measuring the scattering cross section for different bias energies of the detector. From the differences of these cross sections some idea of the spectrum of the scattered neutrons may be obtained.

In the present report measurements on 3-Mev and 1.5-Mev neutrons will be described. Measurements at 0.6 Mev will be reported later.

Two kinds of experiments were carried out: back scattering and transmission experiments.

In the back scattering experiments, a detector is placed between the source of neutrons and a thin disk of the material, and is either shielded from the direct beam by a shadow cone or is made sufficiently directional that this is unnecessary. The detector receives neutrons scattered between some minimum angle θ_{min}, defined by the edge of the disk, and an angle Θ which is equal to π if there is no shadow cone, or is defined by the shadow if there is one. The scattered intensity may be written

$$I = I_0 nx \int_{\theta_{min}}^{\Theta} W(\theta)\ \left[\sigma_e(\theta) + \sigma_i{}'(\theta)\right]\ dw$$

where I_0 is the intensity of the direct beam.

$W(\theta)$ = a weight factor dependent on the geometry, the angular distribution of the source, and the angular sensitivity of the detector.*

$\sigma_e(\theta)$ = elastic scattering cross section per unit solid angle.

$\sigma_i^1(\theta)$ = inelastic scattering cross section per unit solid angle of neutrons which have not lost sufficient energy to be removed from the detectable class. This term can be made small by suitable choice of detector.

n = the number of nuclei per cc in the disk.

x = thickness of the disk.

In the transmission experiments, the disk is symmetrically located between the source and detector. The results are given in terms of an "observed cross section," σ, defined by $I = I_0 e^{-nx\sigma}$, where I and I_0 are the intensities with and without the disk. Assuming a uniform neutron flux incident on all parts of the disk and defining

σ_i^0 = total inelastic cross section corresponding to an energy loss which makes the neutron undetectable,

θ_{max} = the maximum angle through which a neutron may be scattered and still reach the detector,

we may write*

$$\sigma = \int_{\theta_{max}}^{\pi} \sigma_e dw + \int_{\theta_{max}}^{\pi} \sigma_i^1 dw + \int_0^{\pi} \sigma_i^0 dw = \int_{\theta_{max}}^{\pi} \sigma_e dw + \int_0^{\pi} \sigma_i dw - \int_0^{\theta_{max}} \sigma_i^1 dw,$$

where

$$\sigma_i^1 + \sigma_i^0 = \sigma_i$$

The observed cross section, σ, is seen to depend on the detector bias only through the last term. It follows that if the detector is sensitive only to the primary neutrons, σ_i^1 approaches zero and σ is the total inelastic cross section plus the cross section for elastic scattering through an angle greater than θ_{max}. On the other hand, if the detector were equally sensitive to neutrons of all energies

$$(\sigma_i^1 \rightarrow \sigma_i) \text{ then } \sigma = \int_{\theta_{max}}^{\pi} (\sigma_e + \sigma_i)\, dw.$$

It is also evident that the inelastic scattering effect as measured by σ_i^1 will vary directly with the solid angle bounded by θ_{max}. Suitable combinations of differences for various angles and detector sensitivity permit a fairly complete analysis of the scattering and its angular dependence.

A comparison of the results of back scattering and transmission experiments yields a fairly reliable value for the transport cross section and for the cross section for inelastic scattering.

B. BACK SCATTERING EXPERIMENTS WITH DIRECTIONAL DETECTOR AND 3-MEV NEUTRONS

1. Introduction

The elastic reflection of neutrons from the material can be investigated with a detector whose sensitivity is a rapidly increasing function of neutron energy, since such a detector practically does not record neutrons which have lost energy. A thick-paraffin hydrogen recoil is nearly ideal for such measurements since it has a good efficiency, it can be made directional, and it is most sensitive to the neutrons of highest energy. The directional properties of recoil protons eliminates the necessity for a shadow cone usually required to keep the large direct beam from completely masking the small back scattering.

---

*A more complete discussion of these matters will be included in a subsequent paper of this series.

2. Source

The neutrons used for the initial experiments were obtained from the D-D reaction with 50 to 100μa of 200-kv unanalyzed ions on a thick heavy-ice target. The target was cooled with a liquid oxygen refluxing system which has the advantage of requiring only a small amount of material near the target. The neutron intensity was monitored by counting the protons from the companion reaction. The general arrangement is shown in Figure 1.

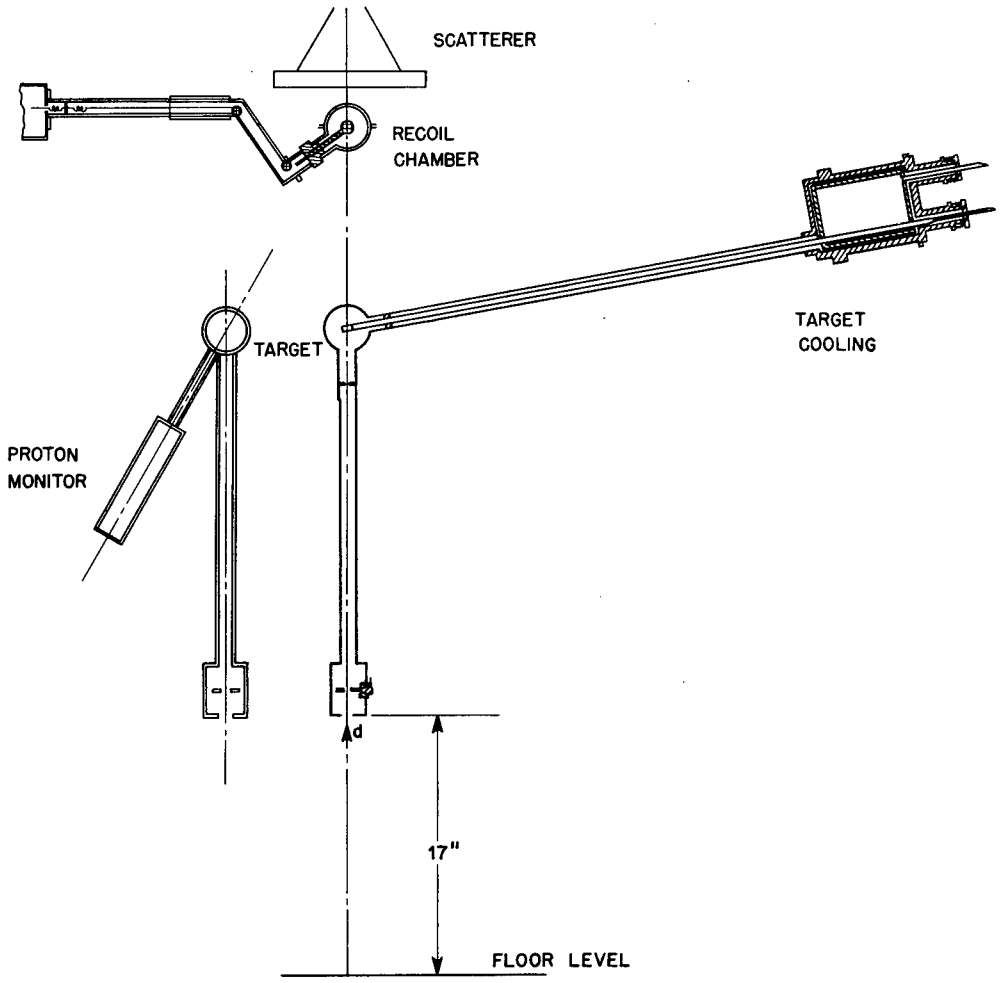

Figure 1.

The deuteron beam was well collimated by two tungsten diaphragms with 3/8-inch diameter apertures in order to locate the source accurately on the target. For the conditions of the experiment, the neutron spectrum rises steeply from 2.5 to 3.1 Mev and then falls abruptly to zero. The energy spread at half-maximum is 10% of the maximum energy.

The angular distribution of this source for the conditions of the experiment is assumed to be $(1 + 0.7 \cos^2\eta)$ in the center of mass system. Experimentally, the counting rate variation from center

to edge of scatterer was found to be less than 10%, in agreement with the above assumption. The half-angle subtended by the scatterer was approximately 17°. The corresponding energy variation is only about 1%.

3. Recoil Chamber

The detector developed for the purpose of these measurements is shown in Figure 2. The chamber was connected to a linear amplifier by means of a coaxial lead about 18 inches long in order to eliminate scattering material in the neighborhood of the chamber. The time of rise of the amplifier was less than 10 microseconds and a short time constant limited the response to motion of the electrons produced by protons in the chamber. With a fast discriminator and a scale of 64, relatively high counting rates were possible with inappreciable loss. The operation of all electrical circuits was frequently checked with artificial pulses. The collection of ions and the corresponding pulse height was periodically investigated with α-particles inserted through the window and with D-D neutron recoils. These recoils were also used to establish the energy scale for the artificial pulses on the assumption of a linear relation between recoil energy and voltage change of the collecting electrode of the chamber. With this scale, the artificial pulses were used to set the discriminator to the desired bias. All pulses greater than this value were recorded.

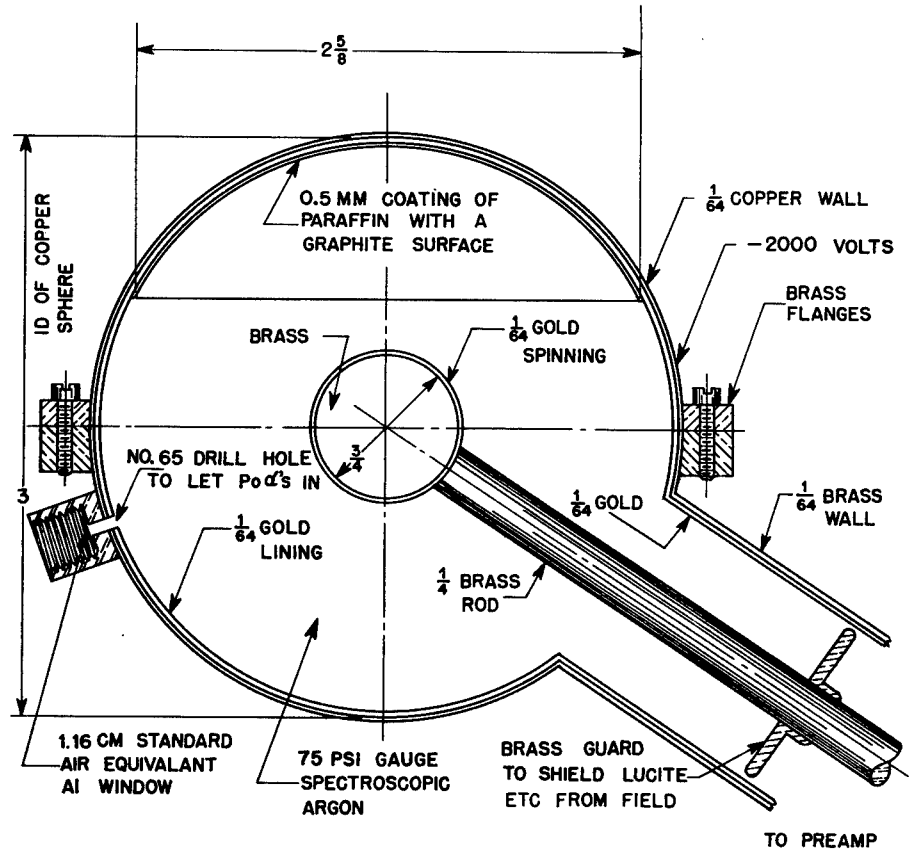

Figure 2.

As first constructed, the chamber was about 20 times as sensitive to neutrons incident on the convex surface of the radiator as for those incident on the concave. A series of investigations as to the origin of the high "background" led to lining the chamber with gold sheet. With such a lining this ratio was approximately 100. The counting rate as a function of the angle of incidence of the neutrons is shown in Figure 3.

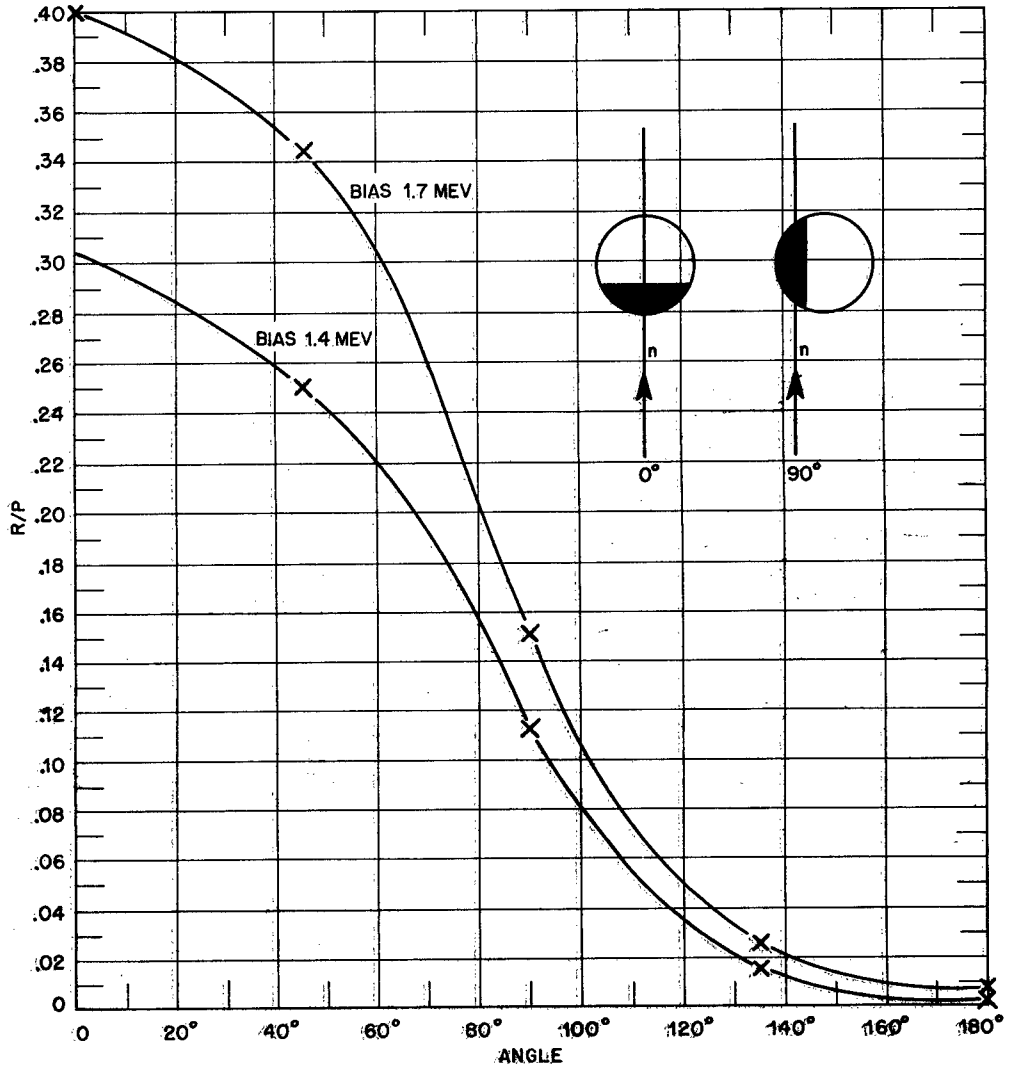

Figure 3. Angular response of recoil chamber.

It was not possible to measure the absolute sensitivity of the chamber for neutrons of energy above the bias energy used, but bias curves were taken for 2.5 and 3.1-Mev neutrons. These curves indicate a reasonable agreement with the response from a thick-paraffin radiator,

$$S \sim E_o^{-\frac{1}{2}} \left[1 - (E_b/E_o)^{3/2}\right]^2$$

which is valid for normal incidence of neutrons of energy E_o on a radiator from which recoils of energy greater than E_b are observed. The geometry and mode of ion collection of the present chamber are not such that more than approximate agreement can be expected.

4. Geometry

In order to specify the geometry, the center of the detector is defined as the point 3/8 inch from the pole of the paraffin cap toward the center of the sphere. Calculations were made to show that this point is quite close to the center of sensitivity of the detector. The position of the scatterer was taken as that of its median plane, and the effect of finite thickness was found to be less than 1%. These points are used to specify the target to scatterer distance, D, and the detector to scatterer distance, δ. Unless otherwise noted, measurements were taken with D = 16 inches; δ = 1 7/8 inches. These dimensions and the scattering disk of 10-inch diameter define a minimum scattering angle of $\theta_{min} = 130°$. The geometric relations involved for this type of back scattering measurement are shown in Figure 4.

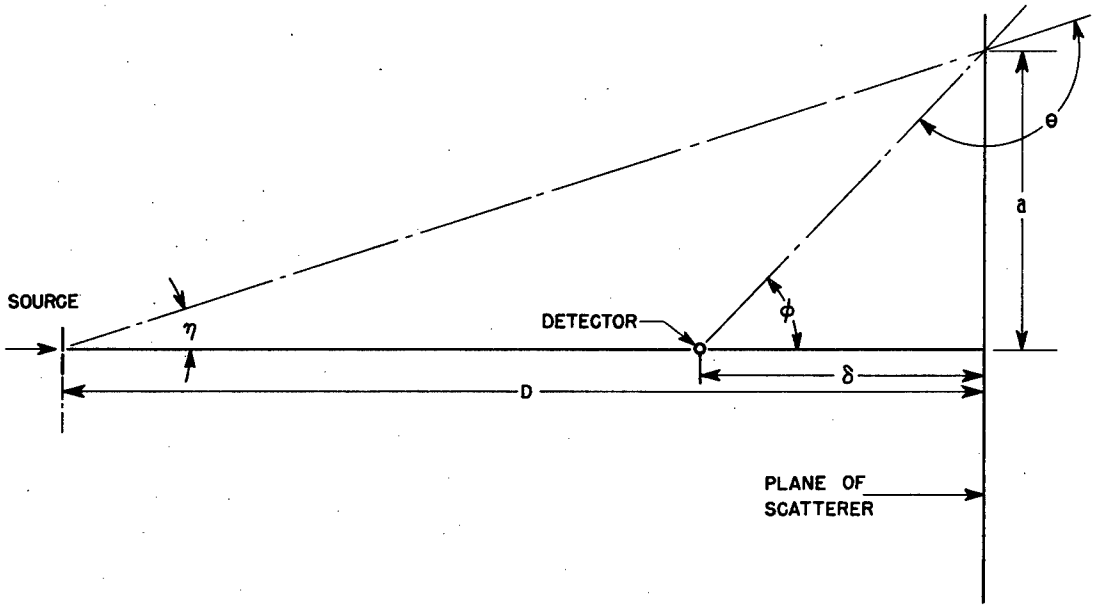

Figure 4. Geometric arrangement for back scattering.

It can be shown* that the counting rate for this case due to the presence of a scatterer of N atoms/cm^2 is given by:

$$C = C_o D_o^2 N \int_{\theta_{min}}^{\pi} \frac{F(\eta)\ \delta(\phi)\ \sigma(\theta)\ dw}{(D-\delta)\ [(Dr/R) - (\delta R/r)]}$$

*Here $(D-\delta) \to 1$, $C_o D_o^2\ F(\eta)\, S(\phi) \to S(\phi,\eta)$, as shown by Olum.[1]

In addition to the quantities defined by Figure 4,

$C_0D_0^2$ = direct beam counting rate times the square of the distance from the source at which it is measured (always at $\eta = 0$).

$F(\eta)$= number of neutrons per unit solid angle from the source, normalized to unity at $\eta = 0$.

$S(\phi)$ = the angular sensitivity of the detector (see Figure 3).

$\sigma(\theta)$ = the scattering cross section per unit solid angle.

$\theta_{min} = \sin^{-1} a(D - \delta)/Rr$

This geometry obviously leads to an average of $\sigma(\theta)$ weighted according to the rest of the intergrand, but since a properly weighted $\sigma(\theta)$ is desired for a transport cross section this may be advantageous. That it is not completely so is illustrated in Figure 5 in which the intergrand, I, for two-disk geometries, as calculated by Olum, and that for the transport cross section are plotted as a function of θ. The rapid rise at the edge of the disk has its origin in the relatively large area subtended by a given $d\theta$ as θ increases in this geometrical arrangement. Questions of intensity and availability of materials precluded a closer adjustment to the desired weighting. The geometric data on the scatterers used are included in Table 1.

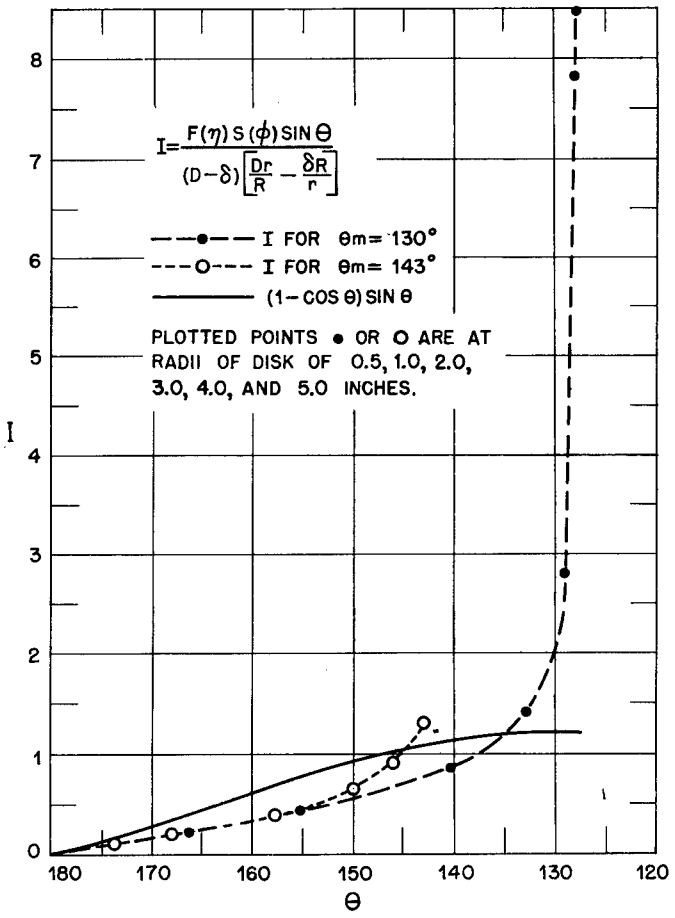

Figure 5. Weight factor for back scattering.

5. Procedure

The counting rate C was obtained as the difference between that with a scatterer in place and with the scatterer removed. For the worst scatterer investigated, the rate with scatterer was about twice that without. C_o was determined by rotating the chamber through 180° to a position on the axis D_o inches from the target. The background for this direct-beam measurement was completely negligible. To secure satisfactory statistical accuracy, most of the total observation time was the time for recording scattered neutrons, since the net rate for the best scatterer was only about 7% of that of the direct beam. All counting rates were related to the proton monitor which had been checked for flatness of bias curve and tested for reproducibility with a BF_3 neutron counter.

Two complete sets of counting rates, C and C_o, were taken according to this procedure for each scatterer. The first corresponded to a bias setting of the detector to record all recoils of energy greater than 1.4 Mev, the second to record all those of energy greater than 1.7 Mev. These values must not be construed as signifying that neutrons down to such energy are detected with nearly the same efficiency as those of higher energy. On the basis of the previously mentioned thick-paraffin sensitivity a rough idea of the sensitivity may be obtained. Since all scattering data were normalized to the direct beam for each bias we may arbitarily take 100 as the chamber sensitivity for 3.1-Mev neutrons. The accompanying tabulation gives the relative sensitivity for neutrons of lower energy.

	Bias, Mev	
Neutron energy, Mev	1.7	1.4
3.1	100	100
2.5	46	38
2.0	14	5
1.5	1	0

This tabulation points out the important fact that at either bias the detector is predominantly sensitive to neutrons which have lost little energy. It was this feature which lead to the use of such a detector.

In tabulating the results (Table 2) obtained from the measurements of C and C_o, it has been assumed that the cross section $\sigma(\theta)$ is constant in the angular range of the integral given above. However, as has been pointed out, the weighting emphasizes the scattering near the minimum angle. To a certain degree, this is checked by measurements on a lead disk and ring, measurements whose difference is not outside the error in each. The results on tungsten carbide for two different minimum angles indicate that at least in this case there is not a significant angular variation. The data of Table 2 are given as $4\pi\sigma(\theta)$ purely for ease of comparison with other total cross sections, even though it is recognized that the scattering is in all probability not spherically symmetric and that the asymmetry depends on the element. No corrections have been applied to the results of Table 2 for energy loss in elastic scattering of the light elements or finite size of detector and scatterer. Olum has examined this last point and has concluded that such corrections are less than 2%.

In view of the supposition that the type of detector used is predominantly sensitive to elastically scattered neutrons for either bias, it is rather surprising to find significant differences in the data taken at the two bias values. In order to see if such effects can be real, the previously mentioned thick-radiator formula was used in combination with energy loss to be expected on classical grounds in aluminum and carbon to calculate the bias effect in these elements. The results are:

	Calculated	Observed
Aluminum	1.11	$1.26 \pm .13$
Carbon	1.43	$1.62 \pm .14$

Since these are in fair agreement for two light elements in which a truly nuclear inelastic scattering is unlikely, significant bias effects for the heavy elements may be assumed to indicate a certain amount

of inelastic scattering. The effect is generally larger in the light elements which is reasonable in view of the detector sensitivity and the fact that inelastic scattering in the heavy elements should give rise to a relatively large energy loss.

As a check on multiple scattering, two thicknesses of iron and beryllium oxide were used, and the data are given for samples 2 and 3 and samples 6 and 7 in Table 2. The data are not sufficiently accurate to be able to state more than that the change in cross section is not unreasonable. The total cross section for iron leads to an expectation of 0.68 for a collision in the one-inch specimen, but this cross section includes small-angle scattering. On the basis of the present differential cross section, assumed isotropic, the probability of a double scattering is only about two per cent. Since similar conclusions can be drawn for the other elements, no corrections for the existence of this effect were applied.

6. Results of Others

Previous investigations of this type are few in number. The data of Wakatuki and Kikuchi[2] cannot be used for comparison since their ionization chamber detector undoubtedly was sensitive to neutrons of lower energy. Their cross section would include more inelastic scattering and therefore be larger than in the present case. Their values of 3.2 for Pb, 1.9 for Fe, and 1.9 for Al consequently may not be considered as in disagreement. The values of Barschall and Ladenburg[3] (Pb, 2.5; Fe, 0.6; C, 1.2; Al, 1.1), on the other hand, should be comparable since these results were obtained by counting helium recoils of energy greater than 1.1 Mev. Dunlap and Little[4] have observed the scattering of 2.5-Mev neutrons by lead, obtaining the spectral distribution with a cloud chamber. They conclude that there is a considerable asymmetric elastic scattering in lead and an inelastic cross section of about 1.5 barns with a most probable energy loss of 1 Mev. The most recent work of this kind is that of Frisch and McKibben,[5] in which the fission of U^{238} was used for detecting the scattered neutrons. Only in the case of lead is there a good agreement. In all other cases the cross sections found in the present experiments are considerably lower. The discrepancy is undoubtedly due both to the difference in energy of the primary neutrons and to the difference in sensitivity of the detector. A possible explanation of the discrepancy is that an appreciable number of inelastically scattered neutrons were counted by the fission detector. This possibility was investigated by observing the relative back scattering of lead and platinum with a hydrogen argon filled chamber. The ratio of scattering of these elements could be varied by changing the bias setting of the detector. At low bias the ratio was found to be even lower than that reported by Frisch and McKibben.[5]

C. BACK SCATTERING, GAS CHAMBER AND 1.5-MEV NEUTRONS

1. Introduction

Back scattering and transmission from some of the scatterers were measured in cooperation with Group P-2, using the Li(p,n) source.

2. Source

The number and energy of the neutrons emitted by this source depend strongly on the angle with respect to the proton beam. As explained in the introduction (Section A), a weight factor has to be introduced if the neutron intensity incident on the scatterer is not isotropic. The corrections applied to the calculated cross sections because of the weight factor may be minimized by a proper choice of the neutron distribution over the disk. This distribution is the one which most closely approximates the case where each annular element of the scatterer receives the same average incident flux. Measurements of the angular variation of intensity were made with the detector at the biases to be used for the scattering experiments. These measurements led to the selection of the angle α between the proton beam and the axis to be used in the scattering experiments. For an angle $\alpha = 40°$, the corrections on account of the anisotropic neutron flux amounted to less than 15 per cent.

The target was about 70 kev thick which produces a spread of 0.08 Mev in 1.5 Mev. The energy varied over the scattering disks, due to the finite angle subtended by the scatterer at the source, between about 1.62 Mev to 1.2 Mev for 90° transmission scattering, 1.6 to 1.3 Mev for 60°, and 1.55 to 1.4 Mev for 30° and back scattering.

The neutron intensity during runs was monitored by a current integrator. All measurements are based on comparisons over a relatively short time, at most an hour. Over much longer times no drift was observed in target strength so that the current integrator was a reliable monitor. A check was made with a BF_3 monitor which also showed the reliability of the integrator as a monitor.

3. Detector

The thick-paraffin radiator, although directional, is not sufficiently sensitive to low-energy neutrons in the presence of those of high energy. The response of a gas chamber or thin-paraffin radiator is much more favorable. Because of intensity considerations a hydrogen-filled ionization chamber was used. This chamber counts reliably recoils due to neutrons down to 500-kev energy.

The chamber was a spherical copper shell, 1/64 inch thick, 3 inches in diameter. The collecting electrode, a ball 1/4 inch in diameter was mounted on a 1/8 inch brass rod in the center of the sphere. The whole interior of the chamber was plated with a .0005 inch-layer of gold to reduce the background. The chamber was filled with 24 pounds of argon and 12 pounds of hydrogen. Under these conditions the range of a 1.5-Mev proton is about one inch.

A negative collecting voltage of about 2100 volts was applied to the copper shell. As in the measurements described in Section B, "electron collection" was used to allow one to use high counting rates.

The interpretation of measurements with any detector involves the knowledge of the sensitivity of that detector for neutrons of various energies. The sensitivity of the chamber was measured, at the biases used for scattering, by changing the energy of the neutrons from the Li(p,n) source from 300 kev to 1.8 Mev. A fission chamber monitored the intensity of neutrons up to approximately 1 Mev. Above this energy the fission count must be corrected for the fission of U^{238}. However, in this region the yield curve for the Li(p,n) reaction, as measured by the c.p. counter, is flat. Therefore, the current intergrator could be used to monitor the intensity above 1 Mev.

The sensitivity of a hydrogen-filled chamber for neutrons of energy E may be calculated readily if the following simplifying assumptions are made: (1) neutrons are scattered by hydrogen isotropically in the center of mass system; (2) recoils of longest range are completely stopped in the chamber; (3) positive and negative ions contribute equally to each voltage pulse. With these assumptions the distribution in energy of the recoiling protons is a constant up to the energy E, and 0 above E. The number of recoils above a given bias energy E_B is:

$$N \sim \sigma(E)\,(1 - E_B/E) \sim E^{-\frac{1}{2}}(1 - E_B/E)$$

The theoretical curves shown in Figure 6 are calculated from this formula. Each of the theoretical curves is multiplied by a normalizing factor to give best agreement with the experimental curves. Calling the normalizing factor at the low bias 1, the factor for the medium bias is 0.65, the one for the high bias 0.39. The deviation of the experimental curves from the theoretical ones is undoubtedly due to the fact that the assumptions (2) and (3) were not fulfilled in the experiments: (2) because of the finite size of the chamber and (3) because "electron collection" was used.

4. Detecting Circuits

The chamber was connected to a preamplifier and linear amplifier as described in Section B.3. The pulses from the amplifier were fed into a three-channel discriminator which permitted the simultaneous counting of all pulses above three biases which could be set independently. The outputs

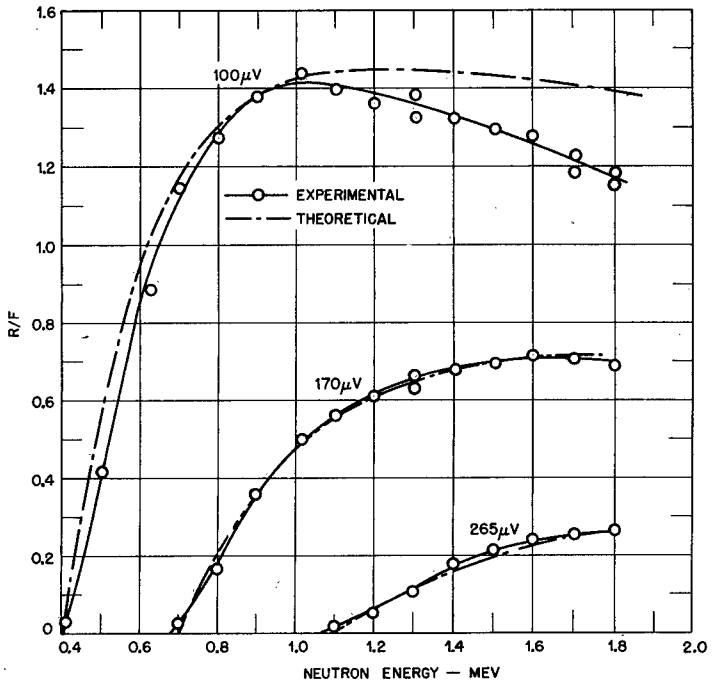

Figure 6. Sensitivity of gas chamber.

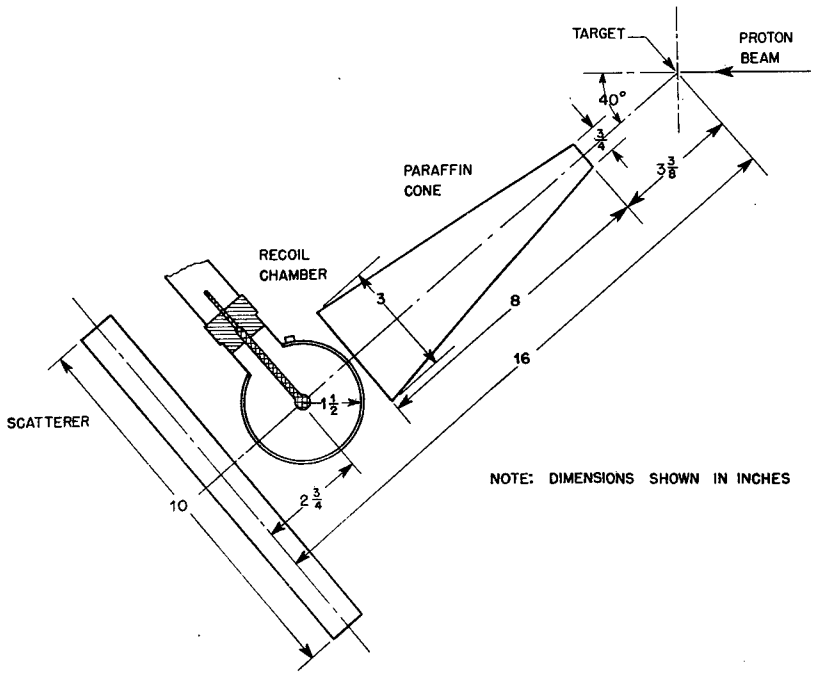

Figure 7. 1.5-Mev neutron back scattering geometry.

of the three channels were fed into three scale-of-64 circuits which operated mechanical recorders. Frequent calibrations were made as described in Section B.3.

5. Geometry—Effect of Shadow Cone

The geometry used for back scattering from disks is shown in Figure 7. Since the gas chamber is not directional, a paraffin cone was used to cut out the direct beam. Consequently, only the outer portion of the disk was illuminated by neutrons from the source. The limiting angles of scattering from the disk are 136° at the outer edge of the disk and 151° at the edge of the shadow. The calculation of the cross section involves the assumptions that the cone does not scatter an appreciable number of degraded neutrons onto the disk, and second, that the cone casts a geometric shadow on the disk. These assumptions require some justification.

The number-bias curve for the neutrons incident on the scatterer was measured by placing the detector in a plane 16 inches from the target, its center 3.85 inches off the symmetry axis. This placed the edge of the detector 1/4 inch outside the geometric shadow of the cone. The measurement was made with the cone in place and without the cone in place. Because of the asymmetry of the distribution, the same measurements were made on both sides of the cone. The neutron count was approximately 3 to 4% higher with the cone in place. One may conclude that there is no appreciable scattering from the cone. The neutron flux incident on the scatterer with the cone in place was measured by moving the detector in a plane perpendicular to the axis 16 inches from the target. These data are shown in Figure 8. The flux without the cone was also measured as a function of angle to the proton beam at a fixed distance from the target. This measurement was made several days later than the experiment with the cone, but the curves for the illuminated part of the disk corrected for $1/R^2$ differences, agree in absolute magnitude to within 5% for all biases. It is also possible to calculate the curves expected in the presence of the cone from those obtained without the cone by assuming a geometric shadow and a given response across the finite size of the detector. The curves thus computed are very sensitive to the assumed response of the detector, but the shadow may be located to within 0.2 of an inch of the geometric shadow for any of several assumed shapes of the response.

These measurements lead one to conclude that the assumption of a shadow 2 inches in radius with no disturbed flux outside, it is a very good approximation. In addition, measurements were made on a Pb ring 7 inches ID, 10 inches OD. The cross section calculated from the Pb ring is in excellent agreement with that calculated from the measurement using a Pb disk.

Rings were also used to measure 90° and 115° scattering. The ring geometries are shown in Figure 9.

6. Procedure

The procedure in taking data was to record recoil counts per monitor count for three conditions, (1) with cone with scatterer, (2) with cone without scatterer, and (3) without cone without scatterer. This gave: $(1)-(2)/(3) = C/C_o$. As in B.4, the cross sections are calculated from

$$\sigma(\theta) = (1/2\pi)\ CD\delta/(C_o n x D_o^{\frac{1}{2}} \int_{x_i}^{x_o} K(r)dr)$$

Where

D = distance between center of target and center of scatterer
δ = distance between center of detector and center of scatterer
D_o = distance between center of target and center of chamber for the measurement of the direct beam (in this case $D_o = l$)
$l = D - \delta$
x_i = radius of the shadow
x_o = outer radius of the scatterer
$\int_{x_i}^{x_o}$ = the integral calculated by Olum from geometry (see Section B.4)

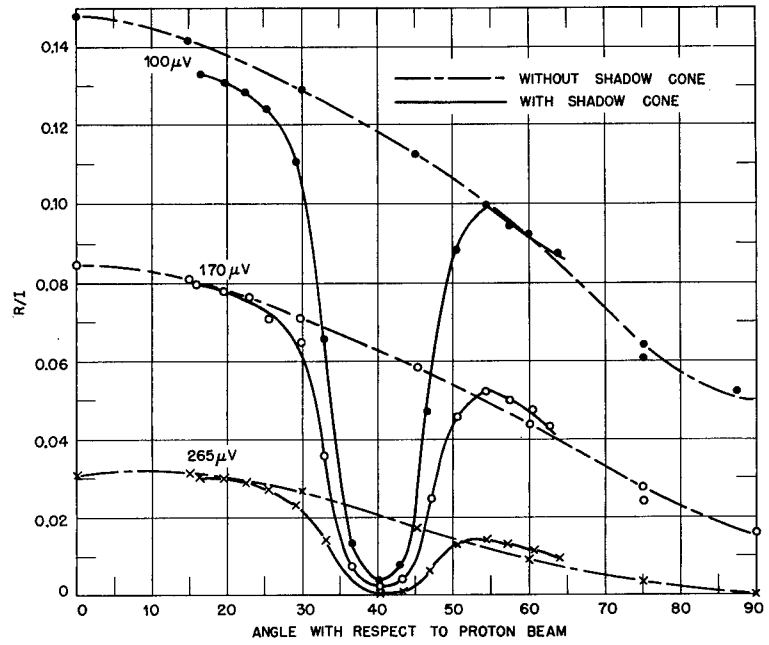

Figure 8. Chamber response.

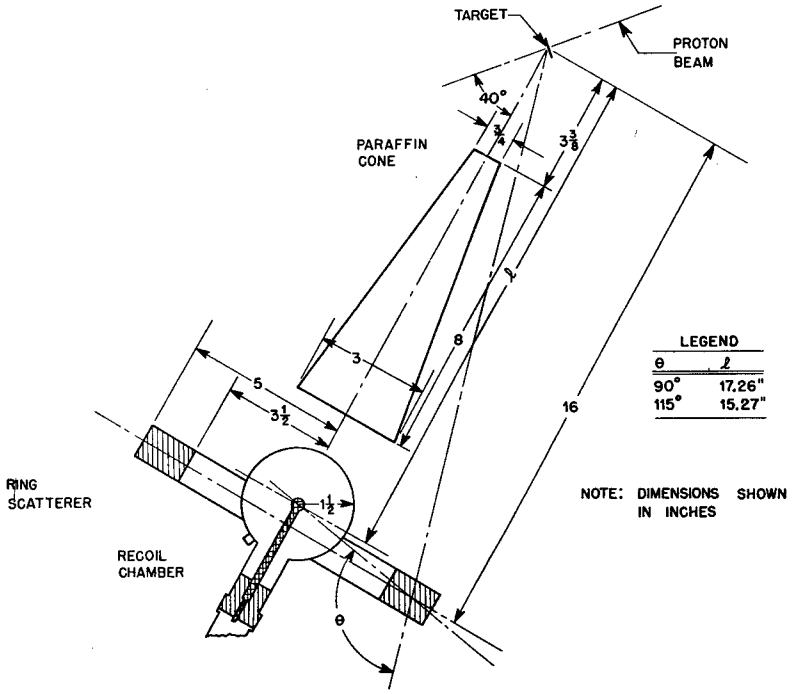

Figure 9. Ring scattering geometry.

For disk scattering, D = 16 inches, l = 13.25 inches, x_i = 2 inches, x_o = 5 inches

For ring scattering, D = 16 inches, l = 17.26 inches for 90°, l = 15.27 for 115°, x_i = 3.5 inches, x_o = 5 inches

This gives the cross section per unit solid angle. These cross sections multiplied by 4π appear in Table 4.

7. Discussion

Pb and W may be compared with measurements with C-d neutrons of 1.6-Mev energy made at Wisconsin (CF-625). These investigations found the following values for $4\pi \times \sigma(\theta)$.

	Wisconsin 138°	High bias, this report 137°	Wisconsin 115°	High bias, this report 115°
Pb	2.29	2.42	3.54	2.82
W	1.29	1.24	1.46	1.30

The combined errors of the two measurements is of the order of about 20% so that the agreement in most cases is satisfactory.

D. TRANSMISSION EXPERIMENTS

Transmission experiments were carried out at 1.5 Mev and 2.8 Mev. The 2.8-Mev neutrons were obtained from the D-D source; the 1.5 neutrons were produced by the Li(p,n) reaction as described previously.

The gas-filled ionization chamber whose properties are described earlier in this report served as a detector. The amplifier mentioned in Section B.3, in connection with the three-channel discriminator (see Section C.4) were used in the transmission experiments.

Figure 10 shows the arrangement used in these experiments. As explained previously, the angle α was chosen in such a way as to make the variation of the neutron intensity (as measured by the detector — to account for energy variation) across the scattering disk as nearly uniform as possible. Measurements of the response of the detector at various angles with respect to the proton beam (see Figure 8) showed that the condition of uniform variation was fulfilled best at 40° for 1.5-Mev neutrons. In the case of the D-D neutrons the known angular distribution of the protons from the D(d,p) H^3 reaction was used for determining the most suitable angle under the assumption that the angular distribution of the neutrons is closely the same as that of the protons. The best angle α turned out to be 60° with respect to the deuteron beam.

Experiments were carried out at various scattering angles θ. The significance of the angle θ is explained in the introduction. The angles θ used were 30, 60, and 90° at 1.5 Mev, and 60, 90, 120° at 2.8 Mev.

The procedure in taking data was to count recoils alternately with and without scatterer. The number of recoils was divided each time by the count of the monitor in the same time interval. Denoting the ratio with scatterer by C, and the ratio without scatterer by C_o, the cross section was obtained from the formula $C = C_o e^{-n\sigma x}$, where n is the number of atoms (or molecules) per cm^3 of the scatterer and x the thickness of the scatterer. The values of σ obtained are shown in Tables 6 and 8. In addition the values of $n\sigma$ are given in Tables 7 and 9.

The results obtained for the 30° geometry (Table 3) should be about 5% lower than "good geometry" measurements. J. H. Williams (CF-507 and CF-599) carried out such measurements at 1.5 Mev and obtained 1.9 barns for carbon. This value may be compared with 1.78 given in Table 8. The difference is not outside the experimental error.

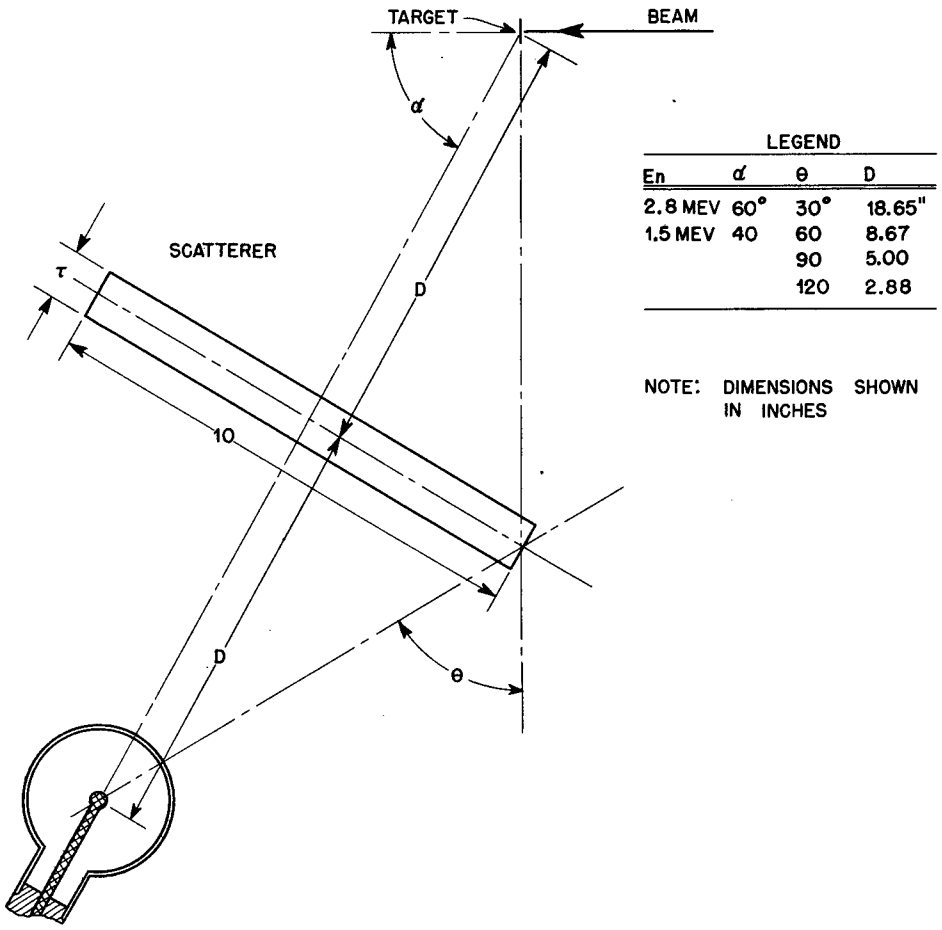

Figure 10.

E. TABLES

In the following tables the cross sections are given in units of 10^{-24} cm^2. In the case of compounds the cross sections are given per molecule. The errors are the average deviations from the mean of the values obtained in individual runs. The tables of the scattering per unit volume are based on extimates of the highest density of the substance which one may expect to obtain. The density used in the calculations agrees only in the case of the metallic samples with the density actually used in the experiments. The cross sections are not corrected for the change in sensitivity of the detector in case of energy loss in the scattering process.

Table 1. Samples used in scattering experiments.

Sample No.	Substance	Mol. or At. Wt. Disks	Thickness of Sample cm	Area cm^2	Mass kg	Density gm/cm^3	Mol. or $At./cm^2$ x 10^{-24}	n x 10^{-24} per cm^3	Optimum Density gm/cm^3	Optimum n x 10^{-24} per cm^3		
1	C	12.0	3.81	506	3.09	1.60	.306	.0804	1.60	.0804		
2	BeO	25.0	6.35	513	5.02	1.60	.235	.0385	2.5	.0602		
3	BeO	25.0	4.37	511	3.91	1.75	.185	.0422	2.5	.0602		
4	Al (dural)	27.9	2.54	506	3.58	2.79	.153	.0623	2.79	.0623		
5	SiC	40.1	4.44	515	3.39	1.48	.0988	.0222	2.5	.0375		
6	Fe	55.8	5.08	506	20.06	7.79	.428	.0840	7.79	.0840		
7	Fe	55.8	2.54	506	10.03	7.79	.214	.0840	7.79	.0840		
8	SiO_2	60.1	6.35	512	5.06	1.56	.0989	.0156	2.6	.0261		
9	Al_2O_3	101.9	6.35	504	4.03	1.25	.0472	.00740	2.8	.0166		
10	W	183.9	2.54	506	21.6	16.8	.139	.0550	16.8	.0550		
11	Pt	195.2	2.54	506	27.6	21.4	.168	.0663	21.4	.0663		
14	Au	197.2	2.54	506	24.9	19.3	.150	.0591	19.3	.0591		
15	Pb	207.2	2.54	506	14.6	11.4	.0836	.0331	11.4	.0331		
		Rings							Optimum Density	Optimum n x 10^{-24}	ID cm	OD cm
17	C	12.0	3.81	258	1.58	1.60	.306	.0804	1.60	.0804	17.8	25.4
18	BeO	25.0	4.37	258	2.01	1.74	.186	.0425	2.5	.0602	17.8	25.4
19	W	183.9	4.37	258	4.37	3.87	.0539	.0149	16.8	.0550	17.8	25.4
20	Pb	207.2	2.54	258	7.45	11.4	.0836	.0331	11.4	.0331	17.8	25.4
21	Pb	207.2	2.54	324	9.36	11.4	.0836	.0331	11.4	.0331	15.2	25.4

Table 2. Back scattering 3.1 Mev.

Sample No.	Substance	σ in barns 1.4-Mev bias	1.7-Mev bias
1	C	.788±8%	.485±7%
2	BeO	.800±7%	.593±9%
3	BeO	.676±6%	.366±7%
4	Al	.661±6%	.525±9%
5	SiC	1.47 ± 5%	1.12 ± 10%
6	Fe	.611±4%	.538±5%
7	Fe	.808±4%	.618±6%
9	Al_2O_3	2.47 ± 5%	2.04 ± 5%
10	W	.382±10%	.349±11%
11	Pt	.472±6%	.441±8%
14	Au	.587±6%	.502±15%
15	Pb disk	2.48 ± 4%	2.29 ± 5%
21	Pb ring	2.26 ± 10%	2.00 ± 10%

Table 3. Back scattering 3.1 Mev. Cross section per unit volume calculated for optimum density of material.

Substance	Optimum density	Optimum $n/cm^3 \times 10^{-24}$	1.4-Mev bias	1.7-Mev bias
C	1.60	.0804	.0633	.0390
BeO	2.5	.0602	.0445	.0289
Al	2.79	.0623	.0412	.0327
SiC	2.5	.0375	.0551	.0420
Fe	7.79	.0840	.0678	.0519
Al_2O_3	2.8	.0166	.0410	.0339
W	16.8	.0550	.0210	.0193
Pt	21.45	.0663	.0313	.0293
Au	19.35	.0591	.0347	.0297
Pb	11.38	.0331	.0821	.0758

Table 4. Back scattering 1.5 Mev (barns).

Sample No.	Substance	90° 100μV .40 Mev	90° 230μV .95 Mev	90° 265μV 1.1 Mev	115° 100μV .40 Mev	115° 230μV .95 Mev	115° 265μV 1.1 Mev	137° 100μV .40 Mev	137° 170μV .70 Mev	137° 230μV .95 Mev	137° 265μV 1.1 Mev
18	BeO ring	2.84 ±1%	1.40 ±5%	0.84 ±8%	2.65 ±1%	0.91 ±4%	0.40 ±8%				
19	W ring	2.58 ±7%	1.78 ±5%	1.38 ±9%	2.81 ±1%	1.94 ±9%	1.78 ±5%				
20	Pb ring	3.06 ±2%	2.53 ±1%	2.38 ±5%	3.97 ±3%	3.50 ±4%	3.17 ±4%				
20	C ring	1.64 ±2%	.86 ±6%	.55 ±6%	1.49 ±2%	.60 ±1%	.28 ±9%				
3	BeO							2.84 ±1%	1.69 ±3%	0.88 ±4%	0.42 ±4%
1	C							1.56 ±4%	1.02 ±3%	.55 ±8%	.22 ±10%
7	Fe							1.93 ±4%		1.28 ±4%	1.10 ±5%
10	W							2.68 ±3%	1.92 ±5%		1.24 ±5%
15	Pb							3.06 ±3%	2.58 ±4%		2.42 ±6%
21	Pb ring							3.05	2.58		2.46

Table 5. Back scattering — cross sections per unit volume for 1.5-Mev neutrons (Calculated for optimum density of material).

Substance	Optimum Density	Optimum $n/cm^3 \times 10^{-24}$	90° 100μV .40-Mev bias	90° 230μV .95-Mev bias	90° 265μV 1.1-Mev bias	115° 100μV .40-Mev bias	115° 230μV .95-Mev bias	115° 265μV 1.1-Mev bias
BeO	2.5	.0602	.171	.0843	.0505	.160	.0548	.0241
W	16.8	.0550	.142	.0979	.0759	.155	.107	.0979
Pb	11.38	.0331	.101	.0837	.0788	.131	.116	.105
C	1.60	.0804	.132	.0691	.0442	.120	.0482	.0225
Fe	7.79	.0840						

Substance	Optimum Density	Optimum $n/cm^3 \times 10^{-24}$	137° 100μV .40-Mev bias	137° 170μV .70-Mev bias	137° 230μV .95-Mev bias	137° 265μV 1.1-Mev bias
BeO	2.5	.0602	.171	.102	.0535	.0253
W	16.8	.0550	.147	.106		.0682
Pb	11.38	.0331	.101	.0854		.0801
C	1.60	.0804	.125	.0820	.0442	.0177
Fe	7.79	.0840	.162		.108	.0925

Table 6. Transmission — scattering cross section for 2.8-Mev neutrons.

A. High bias data		σ (120°)			σ (90°)*			σ (60°)		
Sample No.	Substance	.7-Mev bias	1.4-Mev bias	2.1-Mev bias	.7-Mev bias	1.4-Mev bias	2.1-Mev bias	.7-Mev bias	1.4-Mev bias	2.1-Mev bias
14	Au	1.76 ± 2%	2.72 ± 2%	3.02 ± 3%	2.50	3.03	3.29	3.13 ± 3%	3.53 ± 2%	3.65 ± 3%
15	Pb	.607 ± 50%	1.17 ± 25%	1.58 ± 20%	1.69	1.97	2.47	2.95 ± 2%	3.34 ± 2%	3.87 ± 6%
10	W	1.86 ± 5%	2.87 ± 2%	3.19 ± 8%	1.94	2.66	3.10	2.96 ± 4%	3.37 ± 4%	3.64 ± 10%
11	Pt	1.69 ± 1%	2.54 ± 1%	3.01 ± 1%	2.13	2.76	3.02	2.98 ± 1%	3.29 ± 1%	3.49 ± 1%
5	SiC	.476 ± 2%	.891 ± 4%	1.66 ± 6%	1.24	1.59	2.10	2.40 ± 6%	2.64 ± 1%	2.90 ± 4%
3	BeO	.334 ± 10%	.874 ± 3%	1.55 ± 4%	.982	1.33	1.93	1.59 ± 5%	1.81 ± 5%	2.11 ± 4%
7	Fe	.326 ± 9%	.890 ± 7%	1.34 ± 5%	.657	1.11	1.60	1.32 ± 7%	1.59 ± 2%	1.88 ± 4%
4	Al	.225 ± 40%	.51 ± 20%	.885 ± 10%	.44	.685	1.09	1.26 ± 8%	1.35 ± 3%	1.79 ± 6%
1	C	.039 ± 30%	.385 ± 10%	.765 ± 1%	.525	.695	1.01	.945 ± 3%	1.05 ± 3%	1.12 ± 4%

B. Low bias data*		σ (120°)			σ (60°)			
Sample No.	Substance	250 kev	400 kev	700 kev	250 kev	400 kev	550 kev	700 kev
15	Pb	.13	.30	.49	2.70	2.64	2.78	2.74
10	W		.49	1.87	1.83	2.15		2.95
3	BeO	.02	.08	.22	1.30	1.52	1.73	1.64
7	Fe			.17	1.04	1.17	1.29	1.29
1	C			.12	.81	.83		.86

*No errors are given for the 90° — measurements and the low bias data because the values are based on only one run each.

Table 7. Transmission—cross sections per unit volume for 2.8-Mev neutrons (calculated for optimum density of material).

A. High bias data

Substance	Optimum Density	Optimum n/cm^3 x 10^{-24}	(120°) .7-Mev bias	(120°) 1.4-Mev bias	(120°) 2.1-Mev bias	(90°) .7-Mev bias	(90°) 1.4-Mev bias	(90°) 2.1-Mev bias	(60°) .7-Mev bias	(60°) 1.4-Mev bias	(60°) 2.1-Mev bias
Pt	21.45	.0663	.112	.168	.199	.141	.183	.200	.197	.218	.231
Au	19.35	.0591	.104	.161	.178	.148	.179	.194	.185	.209	.216
W	16.8	.0550	.102	.158	.175	.107	.146	.170	.163	.185	.200
Fe	7.79	.0840	.0274	.0747	.112	.055	.0935	.135	.111	.134	.158
Pb	11.38	.0331	.020	.0385	.052	.0556	.0648	.0816	.097	.110	.127
BeO	2.5	.0602	.0201	.0526	.0932	.0591	.0800	.116	.0957	.109	.127
SiC	2.5	.0375	.0179	.0334	.0623	.0465	.0596	.0787	.0900	.0990	.109
Al	2.79	.0623	.0136	.0307	.0533	.0265	.0413	.0660	.076	.0813	.108
C	1.60	.0804	.0031	.0309	.0615	.0422	.0558	.0811	.0760	.0845	.090

B. Low bias data

Substance	Optimum Density	Optimum n/cm^3 x 10^{-24}	(120°) 250 kev	(120°) 400 kev	(120°) 700 kev	(60°) 250 kev	(60°) 400 kev	(60°) 550 kev	(60°) 700 kev
Pb	11.38	.0331	.0043	.0099	.0161	.0894	.0874	.0920	.0907
W	16.8	.0550		.027	.103	.101	.118		.162
BeO	2.5	.0602	.0012	.0048	.013	.078	.0916	.104	.099
Fe	7.79	.0840			.014	.0874	.0983	..108	.108
C	1.60	.0804			.0096	.065	.067		.069

Table 8. Transmission—scattering cross sections for 1.5-Mev neutrons.

Sample No.	Substance	σ (30°) 100μV 0.4 Mev	σ (30°) 230μV .95 Mev	σ (30°) 325μV 1.3 Mev	σ (60°) 100μV 0.4 Mev	σ (60°) 230μV .95 Mev	σ (60°) 325μV 1.3 Mev	σ (90°) 100μV 0.4 Mev	σ (90°) 230 μV .95 Mev	σ (90°) 325μV 1.3 Mev
10	W	4.45 ±2%	4.95 ±4%	4.97 ±6%	3.00 ±2%	3.56 ±1%	4.16 ±4%	2.06 ±5%	2.99 ±4%	3.43 ±4%
3	BeO	3.29 ±3%	3.46 ±4%	3.52 ±7%	2.02 ±2%	2.56 ±5%	2.94 ±6%	1.18 ±10%	2.04 ±5%	2.76 ±10%
15	Pb	3.36 ±1%	3.54 ±4%	3.68 ±3%	2.43 ±3%	2.64 ±5%	3.05 ±20%	1.72 ±7%	2.01 ±9%	2.00 ±17%
7	Fe	2.25 ±2%	2.46 ±8%	2.56 ±7%	1.59 ±4%	1.87 ±5%	2.02 ±10%	1.03 ±4%	1.47 ±8%	1.74 ±12%
1	C	1.65 ±2%	1.72 ±4%	1.78 ±11%	1.17 ±4%	1.40 ±4%	1.58 ±4%	.641 ±7%	1.09 ±8%	1.36 ±10%

Table 9. Transmission—cross sections per unit volume for 1.5- Mev neutrons (calculated for optimum density of material).

Substance	Optimum Density	Optimum $n/cm^3 \times 10^{-24}$	nσ (30°) 100μV 0.4 Mev	nσ (30°) 230μV .95 Mev	nσ (30°) 325μV 1.3 Mev	nσ (60°) 100μV 0.4 Mev	nσ (60°) 230μV .95 Mev	nσ (60°) 325μV 1.3 Mev
W	16.8	.0550	.245	.272	.273	.165	.196	.229
Fe	7.79	.0840	.189	.206	.215	.134	.157	.170
BeO	2.5	.0602	.198	.208	.212	.122	.154	.177
C	1.60	.0804	.133	.138	.143	.0940	.112	.127
Pb	11.38	.0331	.111	.117	.122	.0805	.0875	.101

Substance	Optimum Density	Optimum $n/cm^3 \times 10^{-24}$	nσ (90°) 100μV 0.4 Mev	nσ (90°) 230μV .95 Mev	nσ (90°) 325μV 1.3 Mev
W	16.8	.0550	.113	.165	.188
Fe	7.79	.0840	.0865	.123	.146
BeO	2.5	.0602	.0710	.123	.166
C	1.60	.0804	.0515	.0876	.109
Pb	11.38	.0331	.0569	.0665	.0662

REFERENCES

1. Olum, LA-45.
2. Wakatuki and Kikuchi, Proc. Phys. Math. Soc., Japan, 21:656 (1939); 22:430 (1940).
3. Barschall and Ladenburg, Phys. Rev. 61:129 (1942).
4. Dunlap and Little, Phys. Rev. 60:693 (1941).
5. Frisch and McKibben, CF-625.

END OF DOCUMENT